Journal of Photochemistry and Photobiology A: Chemistry 221 (2011) 90–97

Contents lists available at ScienceDirect

Journal of Photochemistry and Photobiology A: Chemistry

journal homepage: www.elsevier.com/locate/jphotochem

Improved efficiency of betanin-based dye-sensitized solar cells

Cody Sandquist, Jeanne L. McHale *

Department of Chemistry, Box 644630, Washington State University, Pullman, WA 99164-4630, United States

ARTICLE INFO

Article history:
Received 3 December 2010
Received in revised form 30 March 2011
Accepted 24 April 2011
Available online 30 April 2011

Keywords:
Natural dye sensitizer
Dye-sensitized Solar cell
Betalains
Betanin

ABSTRACT

An improved separation technique employing medium pressure liquid chromatography is used to purify betanin from beet root for use as a sensitizer in a TiO_2-based dye-sensitized solar cell. The use of a blocking layer and treatment by $TiCl_4$ were explored in order to optimize the performance of the solar cell, resulting in energy conversion efficiencies as high as 2.7%, the highest yet recorded for a DSSC containing a single unmodified natural dye sensitizer. The fluorescence spectrum of betanin in aqueous solution is reported as a function of added colloidal TiO_2, demonstrating efficient electron injection. Quenching of betanin fluorescence by TiO_2 permits the observation of its resonance Raman spectrum, reported here for the first time and discussed in light of recent theoretical work on the electronic structure of betanin. We report the results of stability tests under continuous illumination and suggest ways to extend the lifetime of these solar cells.

1. Introduction

Since the first report of dye-sensitized solar cells (DSSCs) in 1991 [1], metal-centered dyes have been the best performing and most widely researched sensitizers, with energy conversion efficiencies as high as 11% [2,3]. Ruthenium-centered polypyridyl metalorganic complexes have been favored in DSSCs because of their strong absorption of visible light, favorable spatial separation of HOMO and LUMO (permitting rapid electron injection and slower recombination), and because they can be repetitively oxidized and reduced without degradation [4]. However, Ru is a rare metal making industrial applications of Ru-based dyes costly and resource limited. Additionally, the environmental and economic costs of using a heavy metal in the DSSC strongly mitigate their main potential advantages over conventional silicon solar cells. The efficiencies of DSSCs containing synthetic organic dyes [5,6] have approached those incorporating metal centered dyes, but synthesis still contributes to the production costs. Ideally, natural plant pigments serving as sensitizers have the potential to improve the economic and environmental benefits of the DSSC, but so far natural dyes have not been able to compete with synthetic dyes in terms of efficiency. Despite lower efficiencies, the benefits of natural dyes will be realized if a greater output of electricity per unit cost can be obtained.

Much of the research on natural sensitizers has focused on either chlorophyll or anthocyanin pigments. These have typically resulted in energy conversion efficiencies of less than 1% [7–10]. Prior to this study, the highest conversion efficiency for a DSSC sensitized with a natural dye, 1.49%, was obtained using chlorophyll-containing extracts from Rhoeo spathacea (Sw.) Stearn ("oyster plant") [11]. Recently, 5.4% conversion efficiency has been obtained by co-adsorption of two synthetic dyes obtained from chlorophyll precursors [12] which were extracted from plants.

Another class of plant pigments with great potential for solar energy conversion is the betalains, consisting of the red betacyanins and yellow betaxanthins. The reddish-purple pigment betanin (Fig. 1) is a betacyanin. Betanin has a maximum absorbance at 535 nm with a molar absorptivity of 65,000 $M^{-1}\,cm^{-1}$ [13]. Betalains are thought to serve the same functions in plants as anthocyanins, acting as "sunscreens" and antioxidants [14–16]. We recently reported the first application of the betalain class of plant pigments in a DSSC, in which red beet root pigments containing betanin were employed to obtain a maximum energy conversion efficiency of 0.67% [17]. In this work, an improved separation method was used to isolate the reddish-purple betanin from the yellow indicaxanthin pigment. The latter is preferentially adsorbed on TiO_2 but has less favorable light harvesting properties [17]. This improved separation of pigments along with efforts to reduce charge recombination has resulted in betanin-based DSSCs displaying efficiencies as high as 2.7%.

The reddish-purple pigment betanin (Fig. 1) is commonly found in beets, bougainvillea flowers and the prickly pear; in most cases coexisting with another yellow or orange betaxanthin dye [15,16]. A recent calculation shows that the visible transition of betanin is well-described as a HOMO → LUMO excitation which moves electron density from the aromatic ring to the dihydropyridyl moiety [18]. The strong absorption of visible light associated with this transition is already taken advantage of the food industry in the use

* Corresponding author. Tel.: +1 509 335 4063; fax: +1 509 335 8867.
E-mail address: jmchale@wsu.edu (J.L. McHale).

1010-6030/$ – see front matter © 2011 Elsevier B.V. All rights reserved.
doi:10.1016/j.jphotochem.2011.04.030

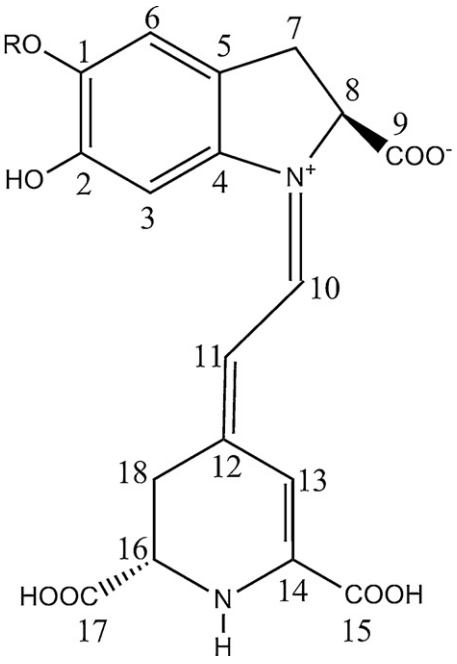

Fig. 1. Structure of betanin. R = β-D-glucose.

of betanin from beets as a food coloring. (The pigment is "generally recognized as safe" by the US Food and Drug Administration.) In previous work, we found that yellow indicaxanthin from beets adsorbs preferentially to the TiO_2 film, limiting the dye-loading of betanin, which has more favorable light-harvesting properties than the yellow pigment [17]. Dye loading of betanin was improved by acid treatment of the TiO_2 film to facilitate adsorption through the COO^- groups on the molecule. In this work, we developed an improved chromatographic method for separating betanin from indicaxanthin and other components of beet extract, resulting in an increased performance of betanin-based DSSCs compared to our 2008 study. Betanin is not available commercially and therefore improved separation of this dye from indicaxanthin in natural materials is an important aspect of optimizing its performance as a sensitizer.

Improved cell performance in this work can also be attributed to efforts to reduce charge recombination (CR). A typical nanoporous TiO_2 film contains numerous surface defects which permit CR to occur at the semiconductor/electrolyte interface [19]. One commonly used method to improve the performance of the DSSC is the post-treatment of the TiO_2 electrode with aqueous $TiCl_4$ [20–22]. The $TiCl_4$ undergoes hydrolysis to deposit nanoparticulate TiO_2 into the film which crystallizes upon sintering. This treatment eliminates defect sites [23] and potentially results in better interparticle connections facilitating electron transport [24]. O'Regan et al. showed that the $TiCl_4$ treatment resulted in a 20-fold reduction in electron–electrolyte recombination [21]. The porosity of the film can also allow the electrolyte to come into contact with the fluorine-doped SnO_2 (FTO) glass anode, permitting electrons from the substrate to recombine with the electrolyte. A common modification to prevent shunting at this interface is the incorporation of a blocking layer [25], in which a thin compact layer of TiO_2 is applied directly on the conductive glass substrate to establish a physical barrier between the substrate and the electrolyte. The importance of a blocking layer is speculated to be greater for comparatively smaller and more planar organic dyes than for the bulkier Ru-centered dyes [26].

It is reasonable to expect that betanin binds to TiO_2 through one or more of its three carboxyl groups. Given the above-mentioned theoretical interpretation of the visible transition, binding through the two carboxylate groups on the dihydropyridyl function would be especially favorable because this would place the LUMO relatively close to the TiO_2 surface and the HOMO farther away, favoring injection over geminate recombination. The resonance Raman spectrum of betanin, which has not been previously reported, has the potential to reveal the nature of its binding to TiO_2. In addition, with the help of the analysis of vibrational modes and their reorganization energies from Ref. [18], the resonance Raman spectrum provides insight into the change in molecular geometry that accompanies electronic excitation. As shown here, however, betanin fluorescence presents a serious obstacle to observing its resonance Raman spectrum. In this work, quenching the fluorescence of betanin not only makes it possible for a resonance Raman spectrum to be acquired, it also reveals efficient electron injection from the dye to TiO_2.

Much is known about the stability of betanin in solution [27–30] due to its use as a food colorant, but no previous research has focused on its long term stability under the conditions it would be exposed to in a DSSC. Factors that contribute to the degradation of betanin in solution include elevated temperatures, exposure to oxygen, light exposure, and pH sensitivity. Betanin is most stable at pH 3.5–5 in aqueous solution [27,28], a pH range in which it exhibits resilience to elevated temperature and light exposure [29]. While the local pH of an acid-treated TiO_2 film is favorable to betanin stability, one must also be concerned with the ability of the molecule to withstand repeated oxidation and regeneration without degradation – a major concern with organic sensitizers. Cyclic voltametry of aqueous betanin reveals three anodic waves at 404, 616, and 998 mV versus Ag/AgCl [30], with the shape of the voltammogram indicating irreversible oxidation. Nevertheless, our previous studies of betanin-sensitized DSSCs suggested that the iodide ion in the electrolyte is capable of regenerating betanin in a working solar cell. Preliminary experiments reported here show that an unsealed betanin-based DSSC can last up to 4 h under continuous illumination with little loss of efficiency.

In this work, we present photocurrent–photovoltage (I–V) and photocurrent action spectra (IPCE) for DSSCs sensitized with purified betanin obtained from beet roots using medium pressure liquid chromatography (MPLC). Resonance Raman and fluorescence spectroscopy are presented and interpreted to gain insight into the excited electronic state structure and efficiency of electron injection into TiO_2. We present the results of stability tests and provide evidence for the potential of betanin to serve as an economical and nontoxic alternative to Ru-centered dyes in DSSCs.

2. Experimental

2.1. Dye extraction and purification

Locally grown beets were purchased from the Farmers Market or the Moscow Food Co-op in Moscow, ID. The beets were peeled, sliced and homogenized in a blender with potassium phosphate buffer, pH 6. Approximately 50–100 mL of buffer solution was mixed with 2–4 beets and blended into a puree. Large solids were separated from liquids by straining the puree through cheesecloth. The juice from the beets was collected and centrifuged for an hour to remove additional solids. The remaining liquid was centrifuged again using Millipore Centriprep Ultracell-3K filters to concentrate the betanin and indicaxanthin pigments and remove high molecular weight components such as starch and proteins. The two pigments were separated using a homebuilt reverse-phase medium pressure liquid chromatography (MPLC) apparatus with Nacalai Tesque's Cosmosil 75C_{18}-OPN as the stationary phase and a mobile phase of 90% water and 10% methanol by volume. The

column length was 30 cm and the flow rate was 18 ml/min. Indicaxanthin elutes first and betanin tends to adhere strongly to the stationary phase unless some methanol is added to the eluant. As described below, pure water was used as the eluant to obtain more pure but more dilute solutions of betanin for fluorescence and resonance Raman experiments. In this case, the betanin fraction was subjected to MPLC a second time, again using pure water as the eluant.

2.2. Fabrication of DSSCs

Surfactant-free TiO_2 films were made from a 1:5 ratio by mass of Degussa P25 TiO_2 in dry ethanol and applied to fluorine-doped SnO_2 (FTO) conductive glass (Hartford Glass) by the method described in Ref. [31]. All films were sintered at 450 °C for 1 h before sensitization. Films made by this method without any additional procedure will be referred to as unmodified films. Two types of film modifications were evaluated. The first was a post-treatment of the TiO_2 electrode with aqueous $TiCl_4$ (Aldrich, 99.9% pure). In this procedure, $TiCl_4$ was added drop-wise to chilled water under stirring to make a solution with a final concentration of 0.1 M. Unmodified TiO_2 films were then soaked in this solution for 12 h under refrigeration before being rinsed with ethanol and sintered at 450 °C for 1 h. The other modification employed was the application of a blocking layer to the FTO glass anode. The blocking layer was made by soaking the bare glass in a 0.1 M solution of $TiCl_4$ for 12 h under refrigeration to deposit a thin TiO_2 layer on the glass surface. The film was then rinsed with ethanol and sintered for 30 min and allowed to cool back to room temperature. After this initial step, a layer of Degussa P25 TiO_2 paste was applied by the doctor blade technique and the film was then sintered at 450 °C for 1 h. The counter electrode was made by drop casting 5 mM H_2PtCl_6 in isopropanol onto FTO conductive glass, evaporating the solvent at room temperature, and then sintering at 450 °C for 30 min. All electrolyte solutions consisted of 0.5 M I_2 and 0.05 M LiI dissolved in either dry 3-methoxyproprionitrile (MPN) (Acros, 98% pure) or acetonitrile (ACN) (Acros, 99.9% pure) solvents. The TiO_2 films were sensitized by first being soaked in an acidic solution of 0.5 M HCl in dry ethanol for 1 h before immediately being transferred into a solution of purified betanin for a minimum of 1 h at room temperature or overnight under refrigeration. Films can be stored in this way for several days.

2.3. Absorbance measurements

A Shimadzu UV-2501 spectrometer was used for absorption studies, a water reference was used for spectra of solutions or an unsensitized TiO_2 film as a reference for transmission spectra of betanin on TiO_2. For measuring the absorption spectrum of sensitized films, a more dilute paste was made from a 1:12 (w/w) ratio of Degussa P25 TiO_2 to dry ethanol, in order to make thinner, more transparent films than those described above. The diluted paste was applied to a quartz substrate by the doctor blade technique. The 75 mm × 25 mm films were cut in half, one half was sensitized with betanin dye while the other half was used as a reference for absorption spectroscopy to attempt to subtract out the extinction due to scattering by TiO_2. Sensitized betanin was exposed to the air for no more than 5 min while the absorbance was being measured. The absorbance of betanin on a film of regular thickness (~10 μm) was also measured using a diffuse reflectance set-up on a PerkinElmer UV/Vis/NIR spectrometer with a Labsphere Teflon reference reflector (USRS-99-020) with a 99% reflectance factor. Reflectance (R) was converted to absorbance using $\log(1/R)$. Using Eq. (1), the absorbance of an unsensitized TiO_2 film was subtracted from that of a betanin sensitized TiO_2 film to account for scattering and accurately calculate the absorbance spectrum of betanin on a TiO_2 film.

$$\log\left(\frac{1}{R}\right)_{bet} = \log\left(\frac{1}{R}\right)_{bet/TiO_2} - \log\left(\frac{1}{R}\right)_{TiO_2} \quad (1)$$

2.4. Characterization of DSSCs

Current–voltage measurements of DSSCs were made by illumination with 13 mW incident light from a 75 W Xenon Lamp. UV and IR filters were placed in front of the sample and the illumination area was 0.126 cm^2. Current and voltage were measured using a Keithly 2400 source meter, and incident light power was measured using a Melles Griot bolometer. Reported power conversion efficiencies are based on the incident light and are not corrected for the absorption of the FTO glass. Energy conversion efficiencies (η) were calculated by:

$$\eta = \frac{V_{OC} I_{SC} FF}{P_{in}} \quad (2)$$

where V_{OC} is the open-circuit voltage, I_{SC} is short-circuit current density, FF is the fill factor, and P_{in} is the incident light power density.

DSSC longevity was preliminarily tested by continuous illumination in a closed circuit. Because the DSSCs were not sealed, MPN was used as the electrolyte solvent for its low volatility compared to ACN. More MPN electrolyte was added when significant drops of efficiency occurred. Sealed cells were not used in order to avoid sample degradation from the use of hot-melt sealants.

Wavelength-dependent incident photon-to-current quantum efficiencies, IPCE(λ), were measured using a PTI Quanta Master fluorimeter with a 75 W Xenon arc lamp source, following the procedure described in Ref. [17] and using the formula:

$$IPCE(\lambda) = \frac{1240.6 I_{SC}}{P_{in}\lambda} \quad (3)$$

where λ is the wavelength of the incident light in nm, P_{in} is the incident power in watts, and I_{SC} is the maximum current in amps. IPCE measurements were validated by measuring the short circuit photocurrent for cells illuminated at discrete wavelengths of 476.5, 488, 496.5, and 514.4 nm from an air-cooled argon ion laser (Uniphase), using incident light power comparable to that from the fluorimeter source after passing through the excitation monochromator. Fig. S1 of supporting information shows that the IPCE values measured at these wavelengths compare favorably to those from IPCE(λ) measured using the fluorimeter apparatus for three different unmodified betanin-based DSSCs.

2.5. Fluorescence, photoluminescence, and resonance Raman studies

Fluorescence of betanin in aqueous solution was obtained using a PTI Quanta Master fluorimeter with a 5 nm slit bandpass. Betanin samples were purified as much as possible in MPLC using only water as an eluant, causing betanin to stick firmly to the stationary phase for a longer period of time to obtain a higher purity but more dilute solution. The betanin solution was run through the MPLC twice using only water as the eluting species, in each case collecting only the tail end of the separated betanin to ensure maximum purity.

Colloidal TiO_2 was added to betanin solutions to quench its fluorescence. The TiO_2 colloidal solution was made by adding $TiCl_4$ to chilled water drop-wise under stirring. Particle size was confirmed by evaporating a 9.1 mM colloidal TiO_2 solution on a quartz slide followed by atomic force microscopy (AFM), revealing particles to be about 16 nm in diameter.

Fluorescence and *resonance Raman (RR)* studies of betanin-sensitized TiO_2 colloids were excited using a Lexel argon ion laser

operating at 528.5 nm for fluorescence and 514.5 nm for resonance Raman, both at 10 mW. A slightly shorter wavelength was used for the RR measurement to minimize interference from the residual betanin fluorescence. Scattered light was reduced with a notch filter and emission was detected with a single monochromator and CCD detection. The absorbance spectrum of the betanin eluant was measured to determine the concentration. Colloidal TiO_2 was added to the betanin solutions to obtain various molar ratios of betanin to TiO_2 as reported below. Fluorescence spectra were taken with a 1 s exposure time and one accumulation, using magnetically stirred solutions to minimize dye degradation. RR spectra were obtained using a backscattering geometry and solutions with maximum absorbance $A \approx 1$ for a 1 cm path length cell. A molar ratio of 1:100 betanin to colloidal TiO_2 (based on TiO_2 units) was used to obtain sufficient quenching of betanin fluorescence. The suspension of betanin-sensitized colloidal TiO_2 was flowed through a cuvette from a reservoir that was kept chilled in ice-water. Reported RR spectra were obtained by 10 accumulations of 30 s exposure time. Molar concentration of TiO_2 was calculated based on stoichiometric conversion of $TiCl_4$ to TiO_2 and the molar concentration of betanin solutions was determined from the absorption spectrum using a peak molar absorptivity of 65,000 M^{-1} cm^{-1} at 535 nm.

3. Results

3.1. Separation of betanin and indicaxanthin by MPLC

Fig. 2 shows the normalized absorption spectrum of raw beet extract compared to that from solutions of betanin and indicaxanthin obtained from MPLC using 9:1 water:methanol as the eluant. Following Ref. [30], the concentration of indicaxanthin (In) in μM can be found from

$$[\mathrm{In}] = 23.8A_{482} - 7.7A_{536} \quad (4)$$

where A_{482} is the absorbance at 482 nm, and A_{536} that at 536 nm. This equation was used along with the molar absorptivity of betanin (Bt) at 536 nm to find the concentrations of both components before and after MPLC. From the spectra of the raw beet extract shown in Fig. 2, there are 0.6 moles of In for every mole of Bt, before MPLC. After one chromatographic separation with 9:1 water:methanol as the eluant, the concentration of In is reduced by 70% (less than 0.2 moles In for every mole of Bt). Using water as the eluant and running the obtained Bt fraction through the column a second time results in a much more dilute solution of Bt in which 90% of the indicaxanthin has been removed. In this work, we used samples obtained from one-time MPLC with methanol:water for solar cell measurements. The more purified Bt samples obtained by chromatographing twice with pure water as the eluant were reserved for resonance Raman and fluorescence measurements in order to avoid the fluorescence from residual In.

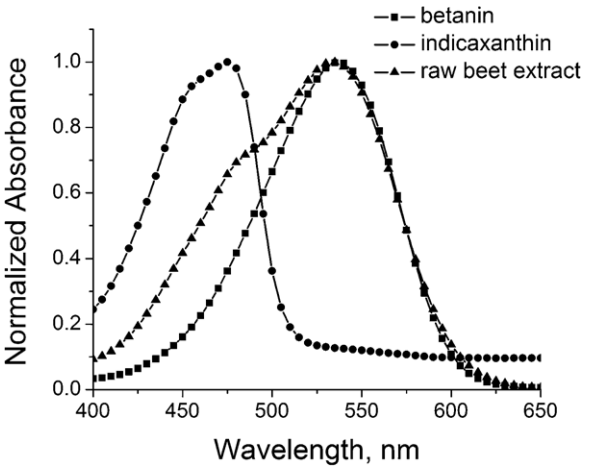

Fig. 2. Normalized absorption spectra of indicaxanthin (circles), raw beet extract (triangles) and betanin purified one time by MPLC using 90% water/10% methanol as eluant (squares).

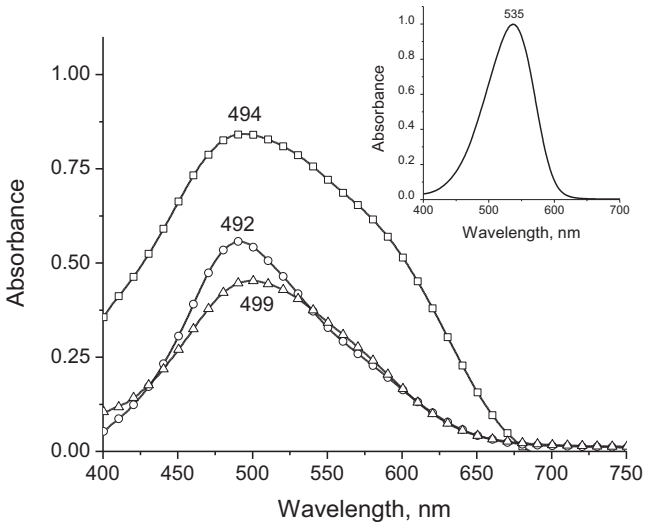

Fig. 3. Absorption spectra of betanin sensitized TiO_2 films. The spectrum of a betanin-sensitized film cast from a dilute TiO_2 paste (1:12 (w/w) ratio of TiO_2 to ethanol) cast on quartz using the doctor blade technique was determined by transmission in either dry ethanol (empty circles) or air (empty triangles). A sensitized film prepared by doctor-blading a paste containing a 1:5 (w/w) ratio of TiO_2 to ethanol, was measured using diffuse reflectance in air (empty squares). The insert is the spectrum of aqueous betanin.

3.2. Absorption spectra

Fig. 3 shows the absorption spectra of two different betanin-sensitized films compared to that of aqueous betanin in the inset. A thin film prepared from a more dilute dispersion of TiO_2 was used to prepare a sensitized film for which the optical spectrum could be measured in transmission. The thin film measurements were made in both ethanol and air environments to judge the contribution of scattering to the measured extinction. The absorbance of a thicker film, comparable to one used in the DSSC, was measured in diffuse reflectance and shows an apparently more extended absorption in the red. The absorption spectrum of the solution phase dye peaks at about 535 nm. In all cases the sensitized films exhibit spectra which are broadened and blue-shifted relative to that of betanin in solution. In our previous work [17], the spectrum of the adsorbed dye was also broadened compared to that in solution, but showed a red-shift. While the origin of this difference is not clear, we speculate that the less pure samples used in Ref. [17] might have resulted in blocking of potential betanin adsorption sites by components of the extract which are not present in this work. Dye absorption on TiO_2 is probably quite inhomogeneous owing to a range of binding sites and binding modes. Many sensitizers are red-shifted on adsorption on TiO_2, and the basis for this blue-shift is not readily apparent and will be the subject for future studies. For example, it could result from the formation of dye aggregates as reported in a carotenoid-sensitized TiO_2 film [32].

The spectrum of the sensitized thin film sample is similar in air and in ethanol, but shows a slight peak shift from 499 nm in air to 492 nm in ethanol. Enhanced scattering contributions from the film in contact with air might have skewed the extinction toward the blue, so we suspect that a solvent effect is responsible for this shift. The diffuse reflectance spectrum of the thicker film matches

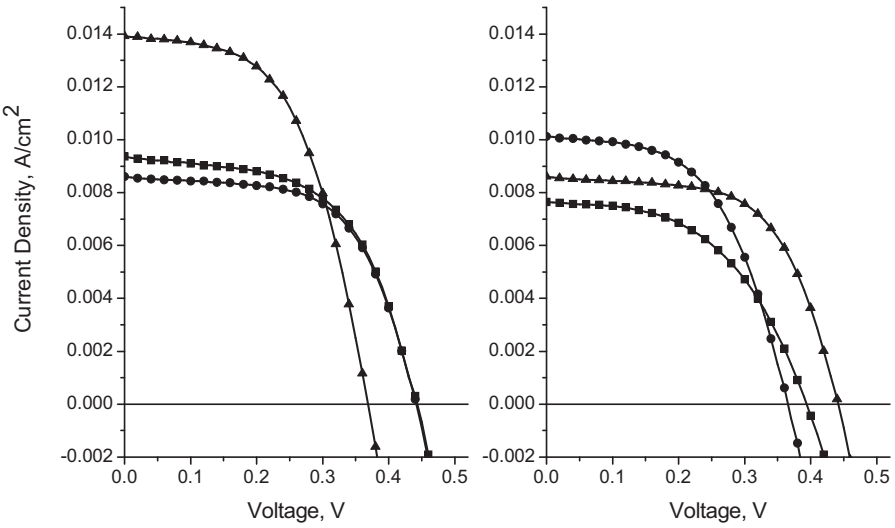

Fig. 4. Comparison of photocurrent versus photovoltage of betanin-sensitized DSSCs using the solvents ACN (left) and MPN (right). DSSCs were made from TiO_2 films that were unmodified (squares), $TiCl_4$-treated (circles), and incorporating a blocking layer (triangle).

the peak absorbance of the thin film in air, but exhibits a spectral broadening and extended response in the red. The photocurrent action spectra shown below exhibit a shape that is close to that of the thick film spectrum of Fig. 3, suggesting the increased breadth of betanin's absorbance on TiO_2 is real and favorable to electron injection at red wavelengths. In all cases, the absorption maximum for betanin on TiO_2 is between 492 and 500 nm.

3.3. Photocurrent and photovoltage measurements

Photocurrent–photovoltage data for DSSCs containing unmodified, $TiCl_4$-treated, and blocking layer films are shown in Fig. 4 and summarized in Table 1. As in DSSCs using Ru-based dyes for sensitizers [33], the best performing solar cells contain either MPN or ACN as electrolyte solvents. In this study, the cells using ACN routinely have a higher η than their MPN counterparts but there is not a clear trend in the I_{SC}, V_{OC}, and *FF* data to account for this. The highest *FF* value of 0.61 was observed in the presence of MPN and a blocking layer, while the highest I_{SC} was 13.9 mA/cm^2 for the blocking layer/ACN DSSC. These I_{SC} values are comparable with those of Ru-based dyes, however, betanin-based DSSCs only have a maximum V_{OC} of 0.44 V, compared to around 0.7–0.8 V for the Ru-based dyes [34]. Since recombination limits both the maximum current and the maximum voltage, higher values of I_{SC} and V_{OC} tend to go hand-in-hand. However, the blocking layer/ACN cell had the highest I_{SC}, but one of the lower V_{OC}'s. Contrarily, the blocking layer/MPN cell had one of the lower I_{SC}'s, but a high V_{OC}. It is feasible that a betanin DSSC could have a relatively high I_{SC} and V_{OC} if recombination could be limited.

Table 1
Comparison of DSSCs.

Electrolyte solvent	Film modifications	I_{SC} (mA cm^{-2})	V_{OC} (V)	*FF*	η (%)
MPN	Unmodified	7.64	0.39	0.51	1.46
MPN	$TiCl_4$	10.13	0.36	0.55	1.93
MPN	Blocking layer	8.61	0.44	0.61	2.22
ACN	Unmodified	10.55	0.35	0.57	2.04
ACN	$TiCl_4$	9.34	0.44	0.57	2.27
ACN	Blocking layer	13.91	0.36	0.56	2.71

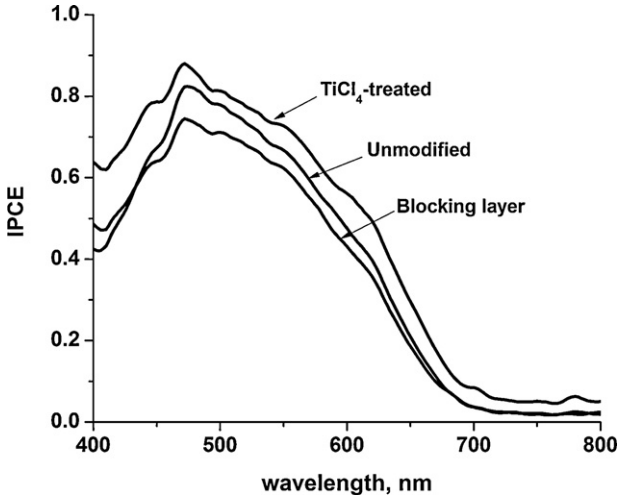

Fig. 5. IPCE(λ) for DSSC's with unmodified and $TiCl_4$ treated TiO_2 electrodes, and incorporating a blocking layer. Electrolyte solution contained I^-/I_3^- in MPN for all samples.

3.4. Incident photon-to-electron conversion efficiencies

Fig. 5 shows the photocurrent action spectra, IPCE(λ), for three DSSCs containing MPN as electrolyte solvent. In this series, the maximum IPCE of about 0.7–0.9 is obtained at the same wavelength, about 490–500 nm, as the peak in the absorption spectrum. The highest IPCE in this series is obtained for the DSSC incorporating a $TiCl_4$-treated TiO_2 film. Some variation in these trends was observed in repeat measurements, as shown in Fig. S2 of supporting information, where a series of measurements resulted in the highest maximum IPCE for a cell with a blocking layer, and the lowest value was obtained using an unmodified film. In this second series, maximum IPCE near unity was observed for the cell incorporating a blocking layer. Note that IPCE values are not corrected for the absorption and reflection of incident light by the conductive glass, which could reduce the incident light power by as much as 20%. The high IPCE values obtained here were unexpected and were therefore checked by measurements at discrete wavelengths using laser excitation as shown in Fig. S1 of supporting information. We have also used the same apparatus to determine IPCE(λ) of an N3-based DSSC. Indeed, in our hands and using the same apparatus,

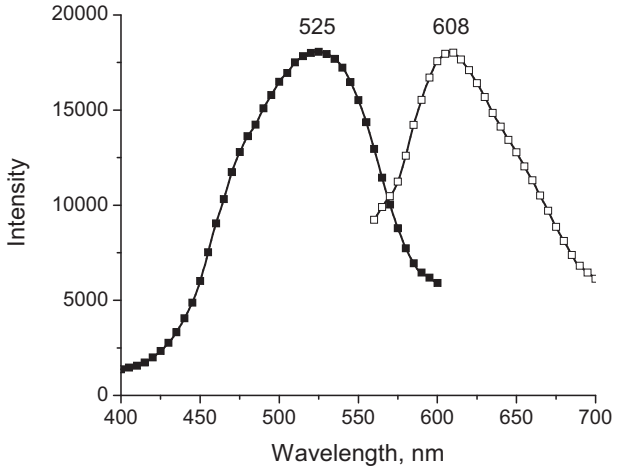

Fig. 6. Emission excited at 535 nm (empty squares) and excitation detected at 610 nm (filled squares) of betanin obtained from beets with residual indicaxanthin present.

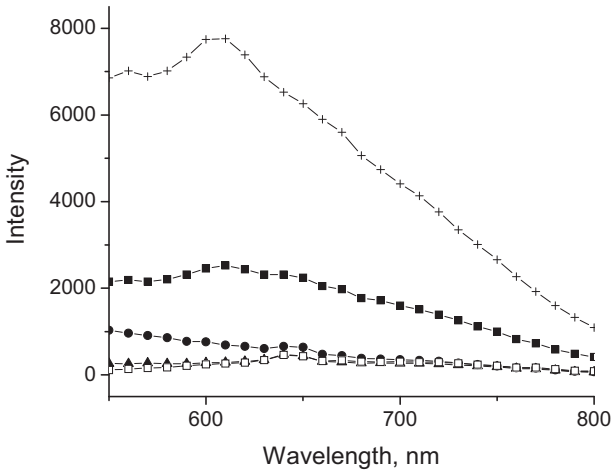

Fig. 7. Fluorescence of betanin in the presence of colloidal TiO_2, with mole ratios of betanin to colloidal TiO_2 1:0 (crosses), 1:5 (filled squares), 1:10 (filled circles), 1:25 (triangles), and 1:100 (empty squares). Excitation wavelength is 530 nm.

the maximum IPCE of an N3-based DSSC (without t-butylpyridine and using an untreated TiO_2 electrode) is only about 60–70%. This can be compared to the reported maximum IPCE for an optimized N3-based solar cell of about 80%, a value which when corrected for absorption and reflection losses of the incident light implies ~100% conversion of photons to electrons near the N3 absorption maximum, according to Ref. [35]. The implications of our IPCE(λ) results for the betanin-based DSSC are discussed further below.

3.5. Fluorescence

Though it has been reported that betanin does not fluoresce [36], we find that purified betanin has significant fluorescence, though it is weaker than that of indicaxanthin. Difficulties in obtaining fluorescence data for betanin by other researchers may be attributed to residual betaxanthin pigment which is much more strongly fluorescent. For this study, as much residual indicaxanthin as possible was removed with MPLC before fluorescence was measured. Fig. 6 shows the excitation spectrum and the emission spectrum of purified betanin in aqueous solution. The former peaks at 525 nm which is close to the absorption maximum of betanin, while the emission peaks at 608 nm. A completely pure sample of betanin would be expected to have an excitation peak closer to 535 nm. Furthermore, the excitation peak is somewhat dependent on the wavelength of the detected emission. For example, when the emission at 790 is detected, the peak in the excitation spectrum peak shifts toward 535 nm. This behavior is the result of the presence of residual indicaxanthin, which makes up about 5% of the pigment content of the twice-chromatographed sample used for fluorescence and Raman measurements.

The small Stokes shift of the fluorescence of betanin makes the measurement of its resonance Raman spectrum difficult. However, using colloidal TiO_2, this fluorescence can be quenched substantially as shown in Fig. 7. The weak peak at 645 nm is from the O–H stretch of water.

3.6. Resonance Raman measurements

The resonance Raman spectrum of betanin adsorbed on colloidal TiO_2 is shown in Fig. 8. Even after a large excess of TiO_2 is added to the betanin solution, the sample is still somewhat fluorescent and a background subtraction of the data is necessary. The peaks labeled in Fig. 8 were obtained reproducibly in replicate experiments. Three prominent peaks at 1387, 1517, and 1603 cm^{-1} are probably characteristic of the aromatic ring. The DFT calculation of Ref. [18] found significant Raman intensity (relative reorganization energy) for a mode calculated at 1603 cm^{-1} and assigned to the in-plane stretching of the C10–C11–C12–C13–C14–C15 chain of the zwitterion depicted in Fig. 1. However, the other two prominent peaks and three smaller ones at 1014, 1115 and 1157 cm^{-1} do not match the theoretical predictions of Ref. [18], thus their assignment is uncertain. The strongest Raman modes were predicted to be low-frequency out-of-plane vibrations which we are unable to detect owing to the notch filter used to reject the scattered laser light. The peak at 562 cm^{-1} is the lowest-frequency peak we observed. To our knowledge, this is the first reported Raman spectrum of betanin. Strong Raman activity of apparent aromatic ring vibrations is consistent with the calculations of Ref. [18], which found that electron density on the aromatic ring contributes strongly to the HOMO.

3.7. Stability tests using continuous DSSC illumination

Fig. 9 shows the results of testing the stability of an unsealed solar cell. Unsealed solar cells were used to avoid the problems associated with hot-melt sealants which can degrade the dye. MPN was used as the electrolyte solvent because it is less volatile than ACN, nevertheless it was necessary to replenish the electrolyte

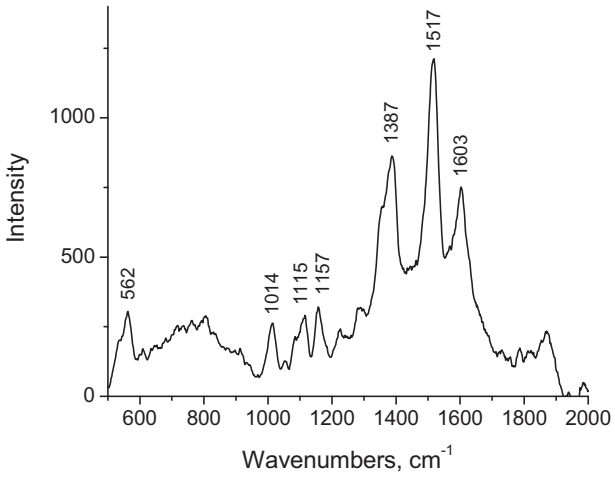

Fig. 8. Background-subtracted resonance Raman spectrum of betanin with 100 times as many moles of TiO_2, excited at 514.5 nm.

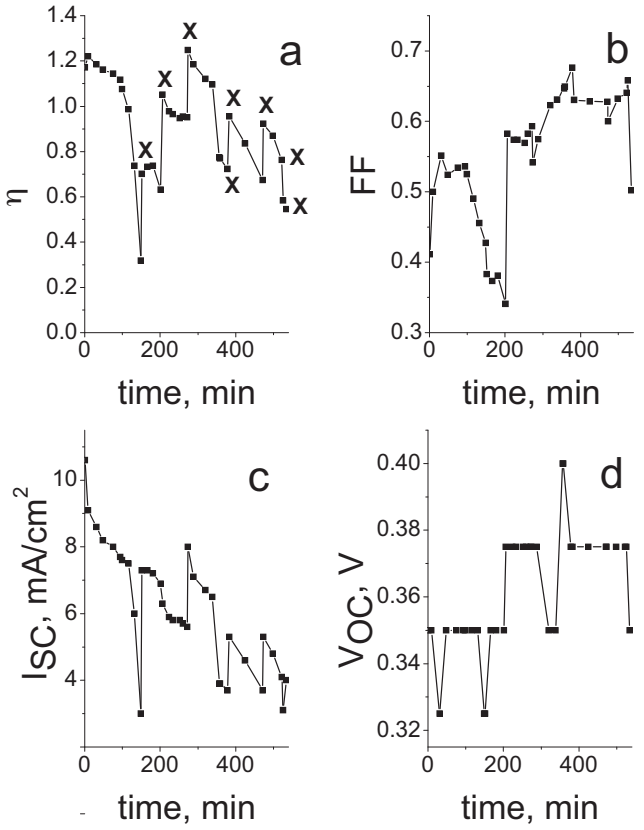

Fig. 9. (a) Efficiency: η, (b) fill factor: *FF*, (c) short-circuit current I_{SC} (A/cm^2), and (d) maximum voltage V_{OC} (V), versus time (min) for unsealed betanin DSSC. Additional MPN (0.5 M I_2, 0.05 M LiI) was added at the times indicated by an X on the η plot.

periodically, as indicated by the X's in Fig. 9. The efficiency and other parameters tended to rebound when electrolyte was added, but a general decline in the efficiency over time was observed. After about 8 h the conversion efficiency was decreased by about 50%. The large dip in η between 100 and 200 min results from solvent evaporation and leads to drops in V_{OC}, *FF*, and I_{SC} that may be attributed to increased series resistance and decreased dye regeneration. This probably results in some irreversible dye degradation, reflected by the steady downward trend in I_{SC} throughout the trial, decreasing at a greater rate than the conversion efficiency. As the I_{SC} decreases, the V_{OC} stays somewhat constant throughout the trial (when solvent is replenished) and the *FF* tends to increase over time. For a reasonable estimate of the dye loading obtained by dye desorption in aqueous base, about 10^{-8} mol/cm^2 (projected area), observed photocurrents of ~10 mA/cm^2 would be sustained for less than ~1 s if the dye were being irreversibly oxidized. Thus it is apparent that the dye can withstand many oxidation–reduction cycles before its eventual decay. The ability to hermitically seal the solar cell will be an important step in future efforts to prolong the lifetime.

4. Discussion

The very favorable photocurrents and IPCE data reported here must be confronted with our low values of V_{OC}. A DSSC based on the widely used ruthenium-based N3 dye [37], for which the maximum photon-to-electron conversion efficiency approaches unity after correction for losses from the conductive glass, can give V_{OC} values as high as 0.7 V and I_{SC} values around 17 mA/cm^2. Our short-circuit photocurrents of ~8–14 mA/cm^2 for the betanin-based DSSC are comparable to those for N3, but much lower values of V_{OC} are obtained. The maximum V_{OC} that can be obtained in the DSSC is set by the difference in the quasi-Fermi level of TiO_2 and the redox potential of the I^-/I_3^- couple, independent of sensitizer. In contact with water, the flat-band potential of TiO_2 is known to shift toward the vacuum level by 0.056 mV for each unit increase in pH, such that a decrease in local pH from about 7 to 1 could possibly account for a decrease in V_{OC} of 0.35 V. However, in several studies using Ru-based dyes, nonaqueous electrolyte, and acid-treated TiO_2 electrodes, acid treatment had little effect on the maximum photovoltage [38,39] or even resulted in a slight increase in V_{OC} [40]. Though these results have been explained by increased electron injection, it is not clear that a Nernstian dependence of flatband potential is valid for a film in contact with nonaqueous electrolyte. The maximum voltage is decided by the relative rates of injection and recombination into the electrolyte according to the equation [41]:

$$V_{OC} = \frac{kT}{e} \ln\left(\frac{I_{inj}}{n\sum k_i [A_i]}\right) \quad (5)$$

where I_{inj} is the rate of (forward) electron injection into TiO_2, n is the surface electron concentration, and the summation is over the rate of electron recombination with oxidized species A_i. For N3 dye, the $Ru^{2+/3+}$ center can provide one injected electron per absorbed photon. Thus maximum IPCE values near unity in the vicinity of the dye absorption maximum indicate that light harvesting, injection, and charge collection are all ~100% efficient at this incident wavelength; hence, recombination is minimal for N3. If we assume, in accord with the results from Refs. [38–40], that the acid pretreatment in our study does not lower the Fermi level of our betanin-based cells, then it is difficult to reconcile IPCE values approaching unity with low and presumably recombination-limited V_{OC} unless the injection efficiencies actually exceed 100%. A two-electron, two-proton process is a reasonable assumption for the oxidation of an organic molecule and would lead to the possibility of IPCE vales greater than unity. It is not clear at this point if this is the case, and further study will be aimed at understanding the oxidation and regeneration processes of betanin in order to optimize its performance and stability in the DSSC.

The resonance Raman spectrum of betanin is reported here for the first time. In accord with the nature of the resonant HOMO → LUMO transition, vibrations of the aromatic ring and conjugated framework are strongly enhanced. Unfortunately, the carboxylate modes are apparently not strongly coupled to the electronic transition and do not show up in the Raman spectrum. Coupled with the inability to obtain a solution phase resonance Raman spectrum owing to fluorescence interference, this prevents conclusions about the binding of betanin to TiO_2 from being drawn in this study.

5. Conclusions

Betanin based dye-sensitized solar cells have improved dramatically from our previous experiments. With a current maximum 2.7% efficiency, betanin is to our knowledge the best performing unmodified natural dye that has been used in a DSSC. The next challenge lies in extending the lifetime of betanin-based DSSCs, focusing in particular on the oxidative and regenerative properties of betanin on TiO_2. Future work will also explore other TiO_2 surface treatments that may allow V_{OC} to be increased by inhibiting recombination in order to maximize energy conversion efficiency η.

Acknowledgments

We are grateful to Prof. Rob Ronald for help with medium-pressure liquid chromatography and Prof. Tom Dickinson for his help in acquiring diffuse reflectance data.

Appendix A. Supplementary data

Supplementary data associated with this article can be found, in the online version, at doi:10.1016/j.jphotochem.2011.04.030.

References

[1] B. O'Regan, M. Grätzel, Nature 353 (1991) 737–740.
[2] Y. Chiba, A. Islam, W. Ashrafal, Y. Watanabe, R. Komiya, N. Koide, L. Han, Jpn. J. Appl. Phys. 2: Lett. Exp. Lett. 45 (2006) L638–L640.
[3] Q. Wang, S. Ito, M. Grätzel, F. Fabregat-Santiago, Iván Mora-Seró, J. Bisquert, T. Bessho, H. Imai, J. Phys. Chem. B 110 (2006) 25210–25221.
[4] M.K. Nazeeruddin, F. De Angelis, S. Fantacci, A. Selloni, G. Viscardi, P. Liska, S. Ito, B. Takeru, M. Grätzel, J. Am. Chem. Soc. 127 (2005) 16835–16847.
[5] T. Horiuchi, H. Miura, S. Uchida, Chem. Commun. (2003) 3036–3037.
[6] H. Choi, J.K. Lee, K. Song, S.O. Kang, J. Ko, Tetrahedron 63 (2007) 3115–3121.
[7] N.J. Cherepy, G.P. Smestad, M. Grätzel, J.Z. Zhang, J. Phys. Chem. B 101 (1997) 9342–9351.
[8] K. Wongcharee, V. Meeyoo, S. Chavadej, Solar Energy Mater. Solar Cells 91 (2007) 566–571.
[9] Q. Dai, J. Rabani, J. Photochem. Photobiol. A 148 (2002) 12–24.
[10] G.R.A. Kumara, S. Kaneko, M. Okuya, B. Onwona-Agyeman, A. Konno, K. Tennakone, Solar Energy Mater. Solar Cells 90 (2006) 1220–1226.
[11] W.H. Lai, Y.H. Su, L.G. Teoh, M.H. Hon, J. Photochem. Photobiol. A: Chem. 195 (2008) 307–313.
[12] X.F. Wang, Y. Koyama, O. Kitao, Y. Wada, S. Sasaki, J. Tamiake, H. Zhou, Biosensors Bioelectron. 25 (2010) 1970–1976.
[13] S.J. Schwartz, J.H. von Elbe, J. Agric. Food Chem. 28 (1980) 541–543.
[14] F.C. Stintzing, R. Carle, Trends Food Sci. Technol. 15 (2004) 19–38.
[15] S. Heuer, S. Richter, J.W. Metzger, V. Wray, M. Nimtz, D. Strack, Phytochemistry 37 (1994) 761–767.
[16] M.R. Castellar, J.M. Obón, M. Alacid, J.A. Fernández-López, J. Agric. Food Chem. 56 (2008) 4253–4257.
[17] D. Zhang, S.M. Lanier, J.A. Downing, J.L. Avent, J. Lum, J.L. McHale, J. Photochem. Photobiol. A: Chem. 195 (2008) 72–80.
[18] C. Qin, A.E. Clark, Chem. Phys. Lett. 438 (2005) 26–30.
[19] Y. Lin, X.R. Xiao, W.Y. Li, W.B. Wang, X.P. Li, J.Y. Cheng, J. Photochem. Photobiol. A: Chem. 159 (2003) 41–45.
[20] C.J. Barbé, F. Arendse, P. Camte, M. Jirousek, F. Lenzmann, V. Shklover, M. Grätzel, J. Am. Ceram. Soc. 80 (1997) 3157–3171.
[21] B.C. O'Regan, J.R. Durrant, P.M. Sommeling, N.J. Bakker, J. Phys. Chem. C 111 (2007) 14001–14016.
[22] N.G. Park, G. Schlichthörl, J. van de Lagemaat, H.M. Cheong, A. Mascarenhas, A.J. Frank, J. Phys. Chem. B 103 (1999) 3308–3314.
[23] F.J. Knorr, D. Zhang, J.L. McHale, Langmuir 23 (2007) 8686–8690.
[24] D.B. Menzies, Q. Dai, L. Bourgeois, R.A. Caruso, Y.B. Cheng, G.P. Simon, L. Spicca, Nanotechnology 18 (2007), 125608 (11pp).
[25] H. Yu, S. Zhang, H. Zhao, G. Will, P. Liu, Electrochim. Acta 54 (2009) 1319–1324.
[26] A. Burke, S. Ito, H. Snaith, U. Back, J. Kwiatkowski, M. Gratzel, Nano Lett. 8 (2008) 977–981.
[27] M.A. Pedreño, J. Escribano, J. Agric. Food Chem. 81 (2001) 627–631.
[28] R. Castellar, J.M. Obón, M. Alacid, J.A. Fernández-López, J. Agric. Food Chem. 51 (2003) 2772–2776.
[29] K.M. Herbach, F.C. Stintzing, R. Carle, J. Agric. Food Chem. 54 (2006) 390–398.
[30] D. Butera, L. Tesoriere, R.D. Gaudio, A. Bongiorno, M. Allegra, A.M. Pintaudi, R. Kohen, M.A. Livrea, J. Agric. Food Chem. 50 (2002) 6895–6901.
[31] D. Zhang, J.A. Downing, F.J. Knorr, J.L. McHale, J. Phys. Chem. B 110 (2006) 21890.
[32] F. Gao, A.J. Bard, L.D. Kispert, J. Photochem. Photobiol. A: Chem. 1330 (2000) 49–56.
[33] J.A. Pollard, D. Zhang, J.A. Downing, F.J. Knorr, J.L. McHale, J. Phys. Chem. 109 (2005) 11443–11452.
[34] V.V. Thavasi, V. Renugopalakrishnan, R. Jose, S. Ramakrishna, Mater. Sci. Eng. R 63 (2009) 81–99.
[35] A. Hagfeldt, M. Grätzel, Chem. Rev. 96 (1995) 49–68.
[36] F. Gandia-Herro, J. Escribano, F. Garcia-Carmona, Planta 222 (2005) 586–593.
[37] M.K. Nazeeruddin, A. Kay, I. Rodicio, R. Humphrey-Baker, E. Müller, P. Liska, N. Vlachopoulos, M. Grätzel, J. Am. Chem. Soc. 115 (1993) 6382–6390.
[38] P. Qu, G.J. Meyer, Langmuir 17 (2001) 6720–6780.
[39] Z.-S. Wang, T. Yamaguchi, H. Sugihara, H. Arakawa, Langmuir 21 (2005) 4272–4276.
[40] K.-H. Park, E.M. Jai, B. Gu, S.E. Shim, C.K. Hong, Mater. Lett. 63 (2009) 2208–2211.
[41] G.J. Meyer, J. Photochem. Photobiol. A 158 (2003) 119–124.